Gold Nanoparticles-Titania Heterojunction: Photoelectrochemical Detection of Ciprofloxacin

Daniele Fumagalli, Silvia Comis, Valentina Pifferi,* and Luigi Falciola*[a]

A photoelectrochemical sensor composed of a heterojunction between titanium dioxide and gold nanoparticles was fabricated and used for the determination of ciprofloxacin, a widely used, but environmentally toxic third-generation antibiotic. This material has been extensively characterized from the morphological, electrochemical and photoelectrochemical points of view, comparing it with the respective counterparts. It has been demonstrated that only the presence of the heterojunction allows the detection of ciprofloxacin, thanks to the properties of gold nanoparticles combined with those of titanium dioxide. These increased performances have allowed the detection of the analyte even with low power sources and wavelengths in the visible region, obtaining good detection limits and excellent resistance to possible interferents. Thanks to this, the future implementation of these sensors in integrated circuits for online and onsite analysis is foreseen.

Introduction

Photoelectrochemical (PEC) sensors have attracted much attention in recent years, due to the numerous advantages such as high stability, fast response, operational simplicity and above all for the reduction of background noise compared to electrochemical and photochemical analyses, thanks to the separation of the excitation source from the detected signal. The core of photoelectrochemical analyses is represented by the photoactive electrode, which must be carefully designed to obtain the best performances.[1–4]

Titanium dioxide was one of the first materials chosen for these analyses, considering its known photocatalytic properties.[5–11] However, this material has some disadvantages, due to the rapid recombination of the photogenerated charges and good activity only under intense UV light. To overcome these problems there are numerous strategies, such as morphological control, doping, sensitization with quantum dots, surface cocatalyst deposition and the formation of heterojunctions. In particular, this last approach has been shown to be very effective,[9,12–16] especially in the case of the formation of semiconductor-metal nanoparticle heterojunctions. The photogenerated electrons can in fact remain in the nanoparticles,

after the transfer through the interface, and the formation of a Schottky barrier turns out to be an efficient electron trap to prevent recombination. Furthermore, if metals with localized surface plasmon resonance (LSPR) properties are used, such as Au and Ag, the absorption in the visible region is also increased.[9,16–20]

One of the fields where these PEC sensors have been applied very recently is the analysis of antibiotics,[2] up to now mainly using systems with recognition elements for the analyte, such as molecular imprinted polymers, aptamers, and enzymes. These systems have the advantage of being highly selective, but facing the drawbacks of more complicated synthetic procedure and storage. Instead, thanks to the intrinsic interaction of the photoactive material with the analyte, without the need for a recognition system, more robust and simpler systems can be built.

Among the antibiotics detected by PEC there is ciprofloxacin,[2,21–25] a third-generation quinolone drug, widely applied for clinical medicine, in livestock and poultry farming, but which has been discovered to be dangerous for the environment even in small quantities, especially for toxicity problems on wastewaters and surface waters. However, these studies are few and above all based on analyses in which the drop in the photocurrent (signal-off type PEC) is observed due to the presence of ciprofloxacin on the surface of the photoelectrode, which hinders the electron transfer.[21–24] This type of detection is more problematic for interferents than a signal-on type PEC, where there is a real chemical reaction between the photoactive material and the analyte and therefore an increase in the photocurrent signal.

In this work, a heterojunction formed by gold nanoparticles coated with a porous titanium dioxide film was investigated for the first time for the signal-on photoelectrochemical determination of ciprofloxacin, using low power light sources. A robust system was obtained, with good analytical parameters and without interference problems. The system was compared with titanium dioxide alone, to fully understand the key role represented by the semiconductor-metal heterojunction.

[a] *D. Fumagalli, S. Comis, Prof. V. Pifferi, Prof. L. Falciola*
Electroanalytical Chemistry Group,
Department of Chemistry,
Università degli Studi di Milano
Via Golgi 19, 20133,
Milano, Italy
E-mail: valentina.pifferi@unimi.it
luigi.falciola@unimi.it
Homepage: sites.unimi.it/ELAN

Results and Discussion

Device Characterization

The final device is composed of gold nanoparticles (AuNPs) covered by a titanium dioxide (TiO_2) layer, as presented in the scheme of Figure 1A (inset). The nanoparticles were obtained with a Turkevic synthesis[26] and were characterized by UV-vis spectroscopy, obtaining the classic 520 nm plasmon band (Figure S1), and by DLS measurements, showing an average size for the nanoparticles of 10 nm (Figure S2). After synthesis, gold nanoparticles were immobilized on a Fluorine doped Tin Oxide conductive glass (FTO), through the use of silanes, as indicated in.[27,28] The TiO_2 powder, previously extensively characterized and used for electrochemical applications [26-29], was subsequently placed by dip coating in a previously prepared sol and the electrode was thus calcined, obtaining a 100% anatase phase film.[27,28] EDX measurements confirm the presence of the elements (Figure S7) in the device. From the SEM image it can be observed that the electrode surface is very uniform (Figure 1A) and the average roughness obtained at the AFM is (8.6 ± 0.9) nm (Figure 1A, inset).
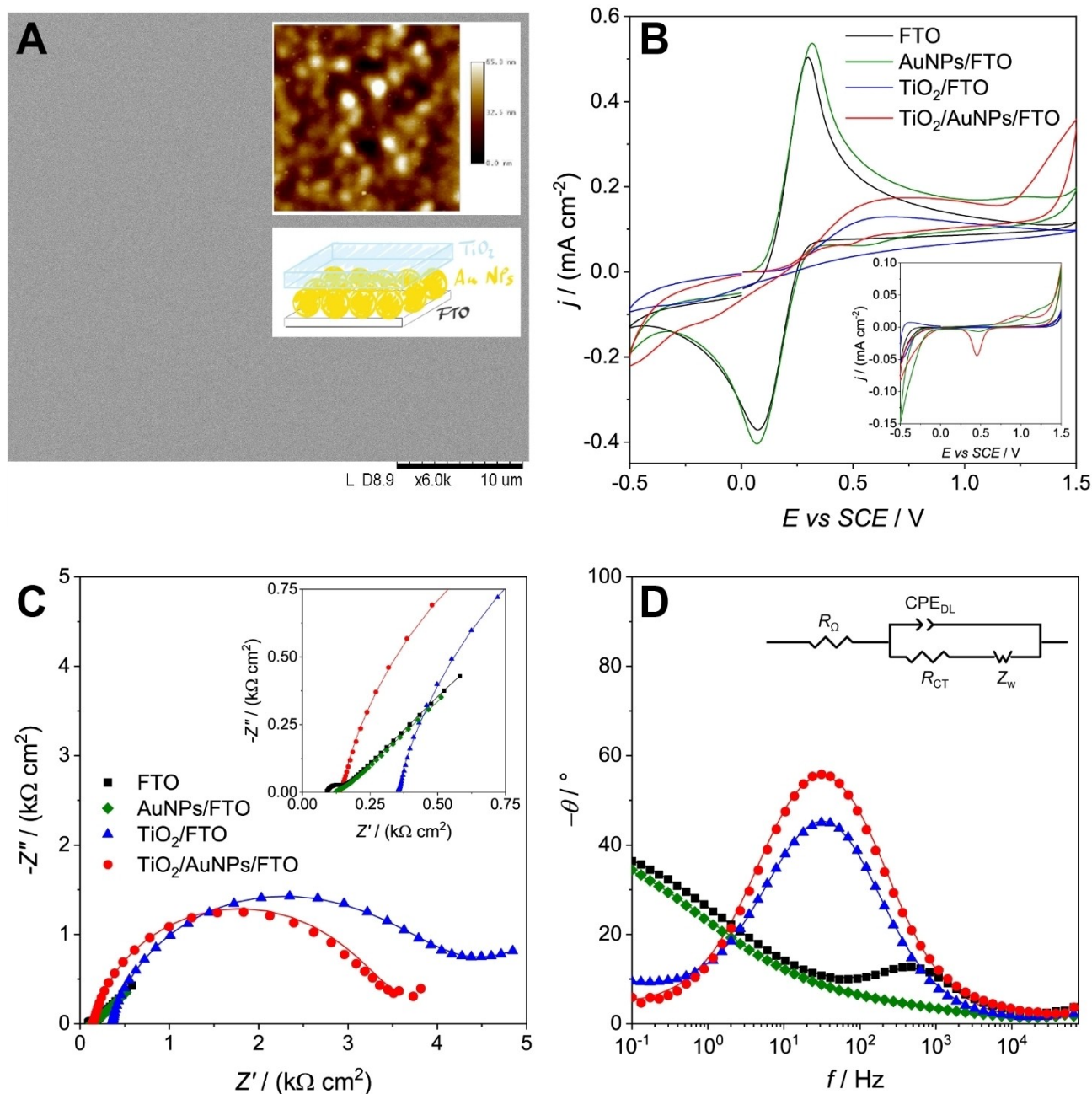
Figure 1. (A) SEM image, AFM and scheme of TiO_2/AuNPs. Cyclic voltammograms at 100 mV s^{-1} (B), complex plane plots (C) and Bode phase plots at +0.25 V (D) registered in 0.1 M $NaClO_4$ in the presence of 3 mM $[Fe(CN)_6]^{4-}/[Fe(CN)_6]^{3-}$ for FTO, AuNPs, TiO_2 and TiO_2/AuNPs. Cyclic voltammograms in 0.1 M $NaClO_4$ without the probe, magnification of complex plane plots and equivalent circuit are shown in insets of B, C, D, respectively.

The device (TiO_2/AuNPs) was electrochemically characterized by Cyclic Voltammetry (CV) and Electrochemical Impedance Spectroscopy (EIS), also considering the comparisons with the individual components: only conductive glass (FTO), gold nanoparticles deposited on FTO (AuNPs) and titanium dioxide deposited on FTO (TiO_2).

Cyclic voltammetry performed on the electrolyte solution without the presence of molecular probe (Figure 1B, inset) shows that FTO and TiO_2 show no signal, as expected, while AuNPs and TiO_2/AuNPs present the typical oxidation plateau and the reduction peak of gold. The latter are very evident, especially for TiO_2/AuNPs, indicating a stabilization and a better electrochemistry of gold nanoparticles after coverage with titania layer. It is also important to consider that this coverage inhibits the loss of gold in solution during the analyses, as instead happens for AuNPs (Figure S3).

Cyclic voltammetry performed in the presence of $Fe[CN_6]^{4-}$/$Fe[CN_6]^{3-}$ as probe molecule (Figure 1B) shows the typical peak signals for FTO and AuNPs, slightly more intense when gold nanoparticles are present. For TiO_2 and TiO_2/AuNPs, on the other hand, the signal appears to be a step, indicating that a different diffusion mechanism is present when the titania layer covers the electrode. In fact, it appears to be porous, as previously demonstrated,[27–29] and confirms the presence of a convergent diffusion mechanism. The convergent diffusion is also confirmed by the study of the scan rates,[30] which shows a slope of the logarithmic graph (Table 1, 2nd column) that deviates from the typically planar diffusion value of 0.5 for the two samples covered by titania. Moreover, the faradic current is higher for TiO_2/AuNPs than for TiO_2, since the presence of gold helps the probe reaction.

Electrochemical impedance spectroscopy performed in the presence of the probe molecule (3 mM $[Fe(CN)_6]^{4-}$/$[Fe(CN)_6]^{3-}$) shows a similar trend in the complex plane plot for all samples (Figure 1C), with a semicircle at high frequencies and a line at low frequencies. This trend is also confirmed by the presence in the Bode plot (Figure 1D) of a peak for all samples. The fitting circuit is the typical Randles circuit (Figure 1D, inset), composed by the cell resistance R_W in series with the electrical double layer capacitance CPE_{DL} and the charge transfer resistance R_{CT}

(in series with an open Warburg element, Z_W), respectively in parallel. The electric double layer capacitance was fitted with a constant phase element (CPE), since the electrode surface is not completely homogeneous, and it is higher and more inhomogeneous (a_{DL} further from 1) for AuNPs (Table 1, 3rd and 4th columns), as expected. The R_{CT} values are instead very low for FTO and AuNPs, since they are completely conductive surfaces, while they obviously increase for TiO_2/AuNPs and TiO_2, recording the highest value for TiO_2. These results are also visible by observing the diameter of the semicircle in the complex plane plot (Figure 1C) and the frequency of the peaks in the Bode plot (Figure 1D), since the higher the frequency, the easier the reaction, and confirm the trend of the peaks in CV (Figure 1B). The analysis of the mass transfer, instead, shows the presence of a very strong convergent diffusion (as previously observed by CV), especially for TiO_2/AuNPs. In this case the lowest value of resistance to mass transfer R_W and a_W are recorded (Table 1, 5th and 6th columns), further from 0.5 (typical of a planar diffusive controlled system), as can also be seen from the Bode graph (Figure 1D).

Photoelectrochemical characterization

Considering that the aim of this work is to use the complete device for photoelectroanalysis, it is also important to carry out a photoelectrochemical characterization by means of electrochemical impedance spectroscopy and photocurrent analysis, comparing especially the samples containing titania.

From the impedance analyses carried out on the electrolyte in the dark or under irradiation, semicircles in the entire frequency range are obtained for all cases in the complex plane plot (Figure 2A). The corresponding circuit (Figure 2B, inset) is composed by the cell resistance R_W in series with the electric double layer capacitance CPE_{DL} and with the film resistance R_F, respectively in parallel. From a first analysis it can be seen that for both TiO_2 and TiO_2/AuNPs systems the diameter of the semicircles (Figure 2A) and the film resistances (Table 2, 5th column) decrease when they are irradiated. This is possible because under illumination the number of charge carriers

Table 1. CV and EIS parameters for FTO, AuNPs, TiO_2 and TiO_2/AuNPs in the presence of $[Fe(CN)_6]^{4-}$/$[Fe(CN)_6]^{3-}$ 3 mM in 0.1 M $NaClO_4$.

	ln(j) VS ln(v)	CPE_{DL} / [$\mu F\,cm^{-2}\,s^{\alpha-1}$]	α_{DL}	R_{CT} / [Ωcm^2]	R_W / [Ωcm^2]	α_W
FTO	0.46	17.4	0.86	56.8	2380	0.500
AuNPs	0.416	1240	0.44	91	8670	0.52
TiO_2	0.38	10.3	0.850	2836	2852	0.19
TiO_2/AuNPs	0.20	15.9	0.860	2836	356	0.11

Table 2. EIS parameters of TiO_2 and TiO_2/AuNPs with and without irradiation, in the absence or in the presence of ciprofloxacin 10^{-5} M in $NaClO_4$ 0.1 M.

	CPE_{DL} / [$\mu F\,cm^{-2}\,s\alpha^{-1}$]		α_{DL}		R_F / [$k\Omega cm^2$]	
	Background	Ciprofloxacin	Background	Ciprofloxacin	Background	Ciprofloxacin
TiO_2/ Dark	12.0	12.6	0.95	0.95	1560	1220
TiO_2 Light	17.8	17.8	0.89	0.89	174	162
TiO_2/AuNPs Dark	11.9	13.7	0.97	0.96	279	48.0
TiO_2/AuNPs Light	18.1	22.3	0.94	0.92	7.38	8.61

ChemElectroChem

Research Article
doi.org/10.1002/celc.202201136

**Chemistry
Europe**

European Chemical
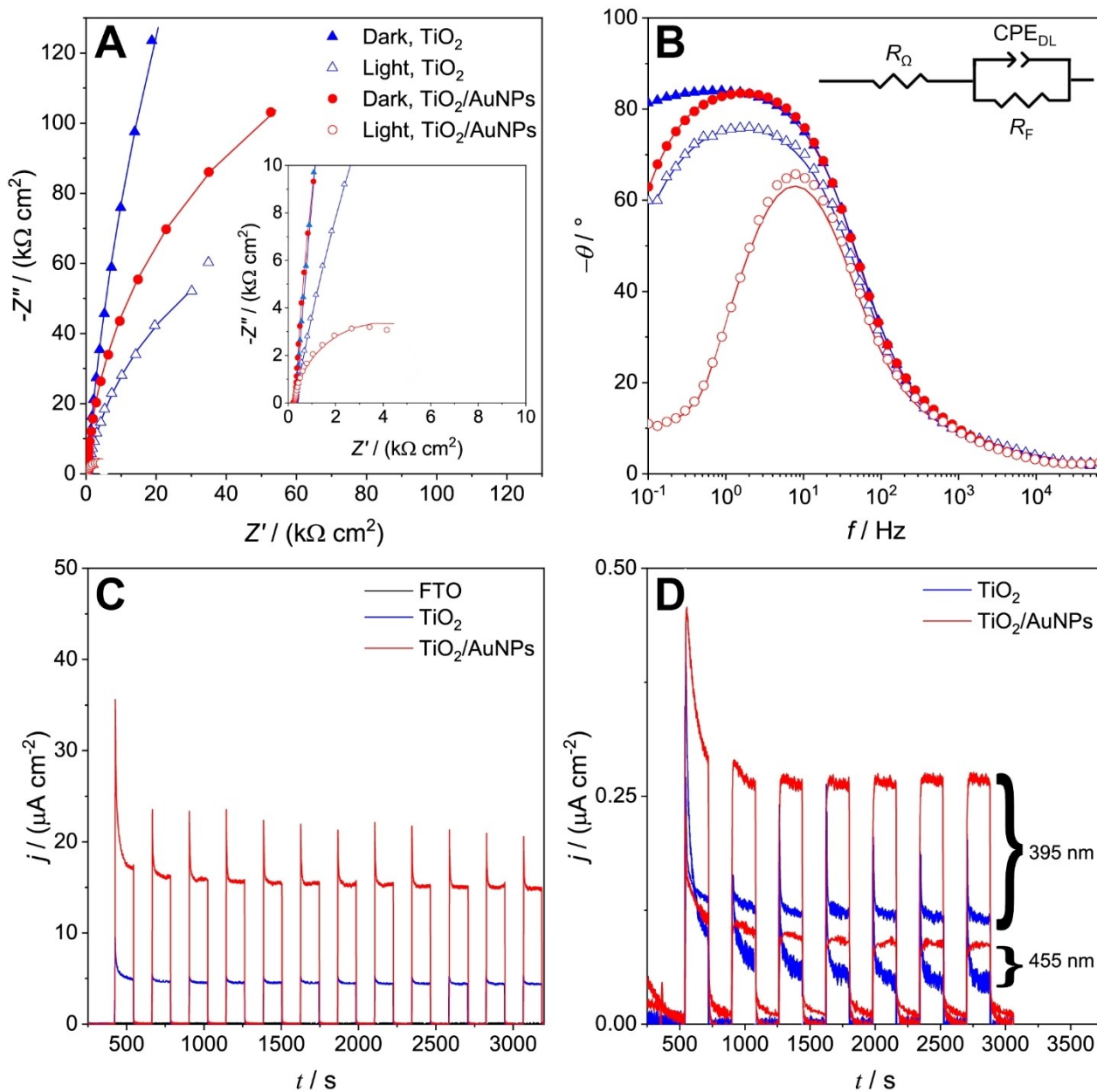Societies Publishing

Figure 2. Complex plane plots (A) and Bode phase plots (B) registered at + 0.1 V in 0.1 M NaClO$_4$ for TiO$_2$ and TiO$_2$/AuNPs in the dark or under UV irradiation with 500 W UV lamp; magnification of complex plane plots and equivalent circuit are shown in insets. Photocurrent measurements registered at + 0.1 V under intermittent irradiation with UV lamp (C) and with LEDs at 395 nm and 455 nm (D).

increases, decreasing the film resistance. However, TiO$_2$/AuNPs already has an order of magnitude lower film resistance in the dark than TiO$_2$, considering the higher conductivity of gold nanoparticles. Furthermore, this resistance drops more strongly, since in this system the charge carriers are more facilitated by the presence of gold. Instead, it is possible to observe how the capacitance of the electric double layer (Table 2, 1st column) under irradiation tends to increase in an identical manner for both samples, since the amount of charges in the capacitor increases in an equal manner, due to titania layer, and is not influenced by the presence of the metal. The major change under illumination for TiO$_2$/AuNPs can also be seen from the

Bode plot (Figure 2B), where the peak becomes very evident and moves to higher frequencies, indicating an increasingly favored process.

The photocurrent tests carried out with the same illumination source employed for EIS (Figure 2C) confirm the results obtained with EIS, showing a current about three times more intense for TiO$_2$/AuNPs compared to TiO$_2$, again showing the excellent conducting action performed by gold.

Moreover, the tests carried out with LEDs at lower power and different wavelengths (Figure 2D) show the best results for TiO$_2$/AuNPs in comparison with TiO$_2$, confirming the responses obtained with a more powerful illumination source. The highest

ChemElectroChem

Research Article
doi.org/10.1002/celc.202201136

**Chemistry
Europe**
European Chemical
Societies Publishing

photocurrent is clearly obtained with the 395 nm LED, while the current is approximately halved for the 455 nm LED.

Considering all the results obtained from the photoelectrochemical characterization, TiO_2/AuNPs can therefore be defined as an excellent candidate for photo-electroanalytical measurements.

Electrochemical impedance spectroscopy was also used in the presence of ciprofloxacin (whose good stability in aqueous solution can be evaluated via UV-Vis spectroscopy – Figure S4), to fully understand the interaction that the molecule can have with the electrodes and with the light. All the samples maintain a trend of the complex plane plot (Figure 3A) and of the Bode

plot (Figure 3B) very similar to the behavior recorded on the background (Figures 2A and B), showing that it is the absence or the presence of irradiation that strongly influences the electrochemical performances. Moreover, the equivalent circuit (Figure 3B, inset) remains the same showed in Figure 2D (inset).

However, small variations in the graphs and fitting values can be observed especially for TiO_2/AuNPs in the presence of the target molecule. In fact, TiO_2 shows identical values of the elements of the equivalent circuit in the dark in the presence and in the absence of ciprofloxacin (Table 2), indicating that in the dark TiO_2 at the applied potential is not affected by the presence of the molecule. When this sample is irradiated, only a
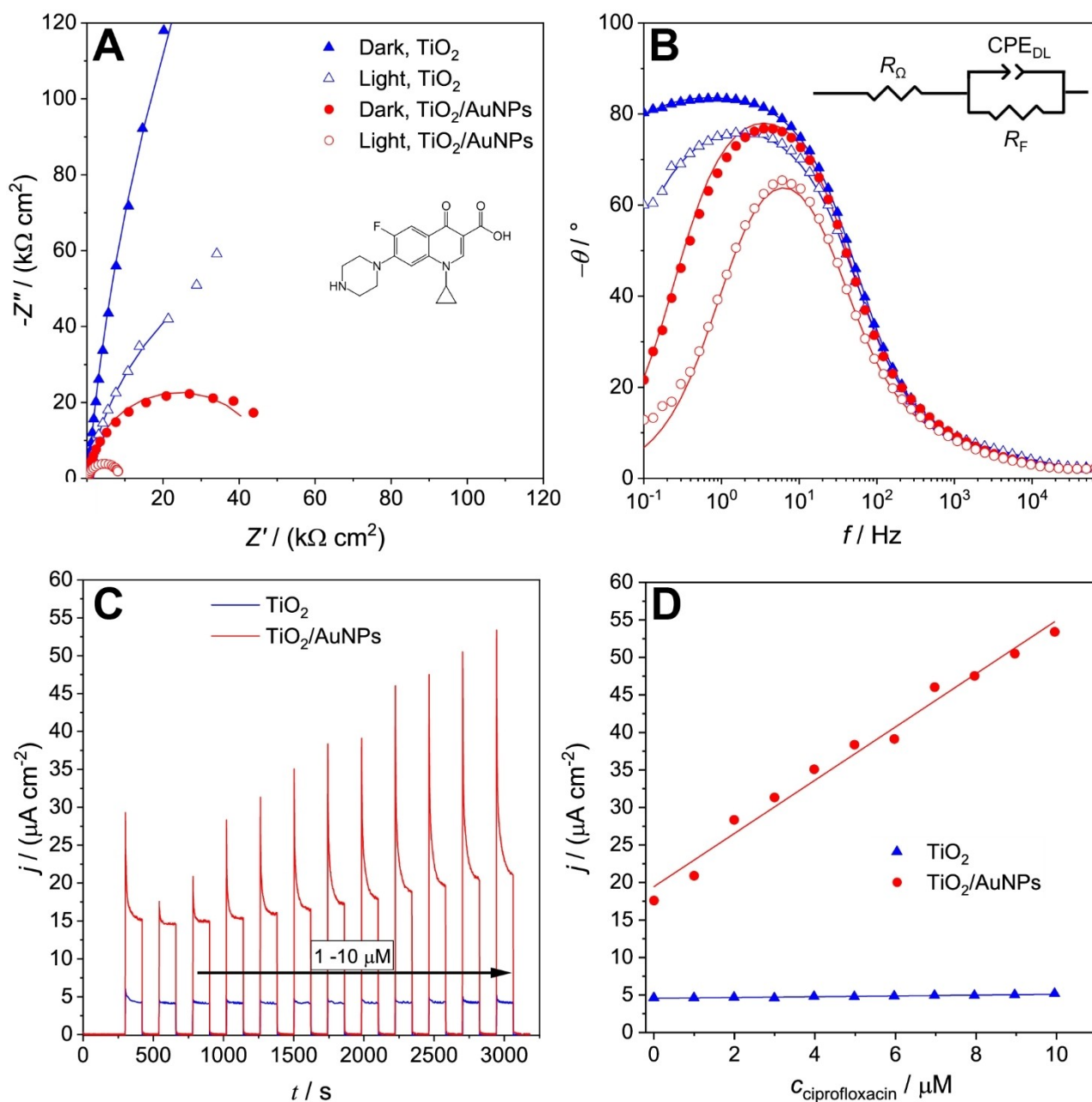

Figure 3. Complex plane plots (A) and Bode phase plots (B) registered at + 0.1 V in 0.1 M $NaClO_4$ in the presence of 10^{-5} M ciprofloxacin for TiO_2 and TiO_2/AuNPs in the dark or under UV irradiation with 500 W UV lamp; equivalent circuit is shown in inset. Photocurrent measurements registered at + 0.1 V under intermittent irradiation with UV lamp for consecutive additions of ciprofloxacin (C) and correspondent calibration plot (D) for TiO_2 and TiO_2/AuNPs.

slight decrease in film strength can be observed, while the other parameters remain unchanged. This demonstrates that light aids the determination of ciprofloxacin, as the film resistance decreases. This fact is also demonstrated by observing the values and behavior of TiO_2/AuNPs in the dark: the resistance of the film also decreases in this case, but much more markedly. This demonstrates that ciprofloxacin can also be determined in the dark, if the resistance of the film is lower, as in this last case. Furthermore, for this sample a small increase in the capacitance of the electrical double layer can also be observed in the presence of ciprofloxacin, which therefore interacts with the electrode surface. When the sample is placed under irradiation there is then a further increase in this capacity, while the resistance remains constant, since it is already a very low resistance.

Ciprofloxacin detection

The previous results confirm the detection tests of ciprofloxacin obtained under irradiation in amperometry (Figure 3C). First, dark tests yielded no results on both electrodes, as the resistances are too high and the applied potential too low for the ciprofloxacin reaction to occur. Under irradiation, on the other hand, ciprofloxacin is oxidized by TiO_2,[31,32] showing an increase in the photocurrent only for TiO_2/AuNPs, demonstrating that only the low resistance of the film obtained by combining gold nanoparticles with titanium dioxide can make the molecule detectable at such low potential. The calibration lines (Figure 3D) confirm the trend observed in photocurrent, showing an increasing trend that is relevant only for TiO_2/AuNPs.

To increase the applicability of the photo-electroanalytical technique, we moved on to the use of less powerful but more manageable lights, deriving from the use of LED sources. Different wavelengths and powers were studied (395 nm, 455 nm and 530 nm) and the best signal was clearly obtained for the LED in the UV at maximum power, even if it is possible to obtain a good signal even at the medium wavelength. The irradiation from the conductive or non-conductive front does not alter the value of the generated photocurrent (Figure S5), while the distance of the source from the electrode is very important, since the generated photocurrent decreases if the distance increases (Figure S6). In Figure 4A the photocurrent obtained under the best conditions is shown and the calibration line obtained several times and on different electrodes is shown in the inset. The analytical parameters are very good and in particular the sensitivity is (1.81 ± 0.04) (μA cm^{-2} μM^{-1}), the limits of detection and quantification (obtained with S/N = 3 and S/N = 10 respectively) are (0.32 ± 0.08) μM and (1.06 ± 0.08) μM, respectively. The precision of the method is very good with a low RSD % ($< 5\%$) and the trueness is also excellent, with apparent recovery factors of 99.8%.

The study of the interferents has considered the possible inorganic and organic contaminants present in surface waters[21–23] where ciprofloxacin can be detected and, as it can be seen from the photocurrents obtained under the same operating conditions of detection of the target molecule (Figure 4B), no detectable interferences were registered.

From the comparison with the literature for the photo-electrochemical determination of ciprofloxacin (reported in Table 3) it emerges that the device presented here is the only one based on a heterojunction formed by nanoparticles of gold and titanium dioxide and above all on a signal-on type PEC obtained through a simple synthesis. Although the detection
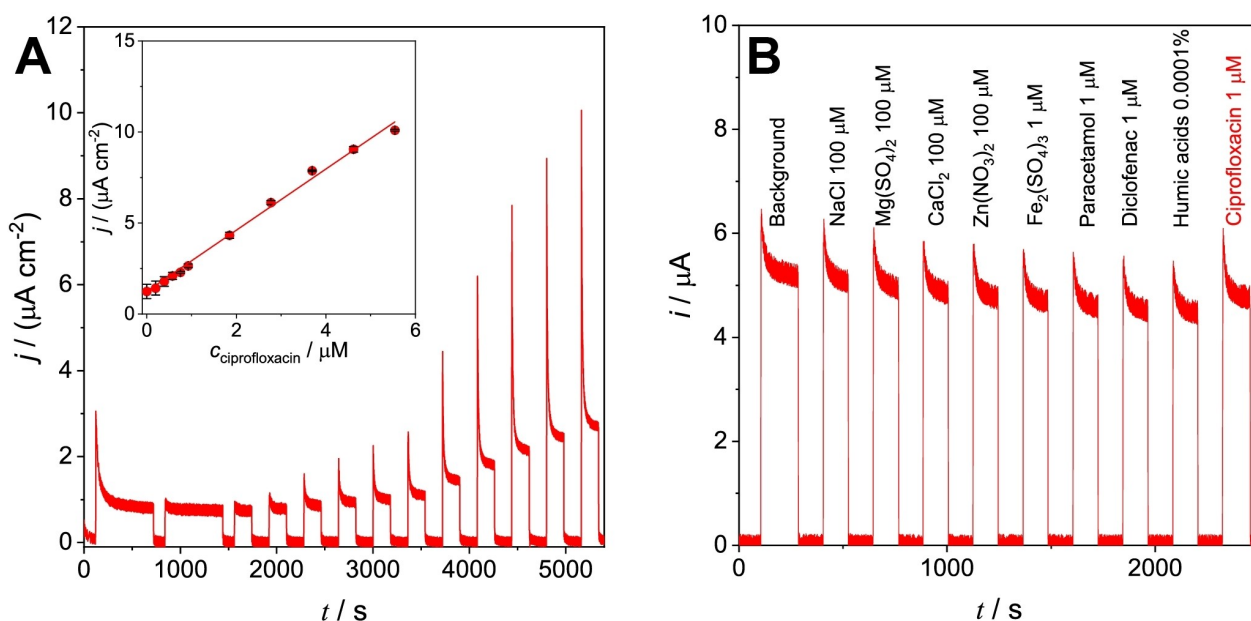

Figure 4. Photocurrent measurements registered at + 0.1 V under intermittent irradiation with a LED at 395 nm for consecutive additions of ciprofloxacin (A) with the correspondent calibration plot in inset and (B) interference study for TiO_2/AuNPs.

ChemElectroChem

Research Article
doi.org/10.1002/celc.202201136

**Chemistry
Europe**
European Chemical
Societies Publishing

Table 3. Sensors for photoelectrochemical detection of ciprofloxacin.

Material	Irradiation	Potential	Signal Type	LOD	Range	Reference
AuNPs/ITO	350 W Xe lamp	0.2 V	Signal-off	0.08 nM	0.1 nM–10 µM	[21]
g-CN/BiOCl	150 W Xe lamp	0 V	Signal-off	0.6 nM	1.5 nM - 5.5 µM	[22]
Bi/BiOBr	150 W Xe lamp	0 V	Signal-off	16 nM	50 nM - 15 µM	[23]
Bi/BiOCl	150 W Xe lamp		Signal-off	0.15 µM	0.5 µM - 30 µM	[24]
ND-g-CN/ITO	300 W Xe lamp	0 V	Signal-on	0.06 nM	0.18 nM – 57.61 nM	[25]
AuNPs/TiO$_2$	395 nm LED	0.1 V	Signal-on	0.32 µM	0.2 µM – 5 µM	This work

limits still have to be improved, it is important to underline that the robustness of the photoelectrode as well as the use of low power LEDs compared to other systems,[21–25] paves the way for the construction of miniaturized systems that can be used for continuous and onsite analysis.

Conclusion

A photoelectrode for photoelectrochemical analysis applications based on a titanium dioxide – gold nanoparticle heterojunction was obtained through a simple and reproducible synthesis. It was characterized by SEM, AFM, CV, and EIS with the presence of a probe molecule and compared with single systems, showing superior electrochemical performances. Subsequently, it was photoelectrochemically characterized by EIS and photocurrent measurements, showing better results than titanium dioxide alone. The presence of metal nanoparticles has in fact proved to be essential to limit the recombination of the photogenerated charges, showing a higher photocurrent and a decreased resistance of the film. In the presence of ciprofloxacin, it has been shown that exclusively the heterojunction allows its detection even using low-power and visible LED light sources, thanks to the low film resistance and to the presence of nanoparticles with localized surface plasmon resonance properties, obtaining good analytical performances and good resistance to interferences. Given the great robustness of the device and the use of more accessible light sources, the application of these systems in integrated circuits for online and onsite analysis is expected in the future.

Experimental Section

Reagents

For the preparation of the TiO$_2$ sol, titanium(IV) isopropoxide (546-68-9), hydrochloric acid 37 % (7647-01-0) and ethanol absolute (64-17-5) were purchased at Sigma-Aldrich, while Lutensol ON70 at BASF.

Gold nanoparticles were prepared using AuCl$_3$ (13453-07-1), trisodium citrate (6132-04-3), PVP10 - Polyvinylpyrrolidone (9003-39-8) and NaBH$_4$ (16940-66-2) purchased at Sigma-Aldrich.

As for the device assembly, FTO (fluorine tin oxide) covered glass slides (7 Ω/sq), acetone (67-64-1), sulfuric acid (7664-93-9), toluene anhydrous (108-88-3), MPTMS - 3-mercaptopropyltrimethoxysilane (4420-74-0) and APTES – 3-aminopropyltriethoxysilane (919-30-2),

where purchased at Sigma-Aldrich while 2-propanol (67-63-0) at Carlo Erba.

Gold nanoparticles preparation

Three solutions containing respectively 0.015 g of AuCl$_3$, 0.022 g of trisodium citrate dihydrate and 0.01375 g of PVP10 in 50 cm^3 of water were mixed in a round-bottomed flask using a mechanical stirrer, and a solution prepared by dissolving 0.001875 g of NaBH$_4$ in 1.25 cm^3 of milliQ water was added dropwise. The solution was left under stirring for 15 minutes, kept at room temperature away from light for a few hours and then stored in a plastic bottle at 4 °C.

SOL preparation

14.2 g of Ti(OiPr)$_3$ were added in a beaker with 50 cm^3 of EtOH. The solution was poured in a 100 cm^3 flask and 0.45 cm^3 of HCl 37 % were added under magnetic stirring. A solution of 0.235 g of Lutensol (a non-ionic surfactant) in 50 cm^3 of ethanol was added in the flask, which was then closed. The solution was stirred for 1 hour and then the sol was stored in glass bottles.

Device assembly

The sensor was prepared on a 2x3 cm FTO support, which was previously sonicated in a 1:1:1 isopropanol:acetone:water solution for 10 minutes, dried with N$_2$ flux and irradiated for 1 hour with a 500 W UV lamp. The cleaned FTO electrode was dipped in a concentrated H$_2$SO$_4$ solution for 90 seconds, then rinsed with water and carefully dried with N$_2$ flux. The electrode was laid in a reactor created ad hoc, with the conductive side on top, with 18 cm^3 of anhydrous toluene. The reactor was carefully sealed and N$_2$ was fluxed for 3 minutes before placing it in a crystallizer with water and kept at 70 ± 5 °C for 1 hour.

A solution made with 2 cm^3 of toluene, 36 mm^3 of MPTMS (3-mercaptopropyltrimethoxysilane) and 4 mm^3 of APTES (3-aminopropyltriethoxysilane) was added in the reactor, which had to be kept at 70 ± 5 °C for another 3 hours.

The electrode was then carefully removed from the reactor, rinsed and sonicated with toluene for 3 minutes. The cleaning procedure was also repeated with ethanol and water, before drying with N$_2$ flow. Such electrode was placed in a petri dish with the conductive side on top and was covered with a gold nanoparticle solution for 1 hour. The excess of solution was later washed away with water, and the surface was dried with N$_2$ flow.

To form the TiO$_2$ film, the electrode was dipped in the TiO$_2$ precursor's sol for 60 seconds, then placed in a glass tube with N$_2$ flux and calcinated in an oven at 400 °C for 1 hour.[27–29,33,34]

All the details concerning the preparation of the TiO$_2$ sol and the preparation and characterization of gold nanoparticles (DLS and UV-Vis studies) are reported in the Supporting Information.

ChemElectroChem

Research Article
doi.org/10.1002/celc.202201136

**Chemistry
Europe**

European Chemical
Societies Publishing

Materials characterization

Atomic Force Microscopy (AFM) images were acquired on a Nanoscope Multimode IIId (Bruker) instrument. Root mean squared roughness (RMS) values were determined on $1 \times 1 \mu m^2$ areas. SEM-EDX images were acquired with a HITACHI TM-1000.

Electrochemical analyses

Electrochemical measurements were performed using a Potentiostat Galvanostat [PGSTAT30] from Autolab, in a standard 3-electrode cell consisting in a platinum wire as counter electrode, the modified FTO glass as working electrode and a Saturated Calomel Electrode (SCE) from Amel as reference electrode. $NaClO_4$ 0.1 M was used as support electrolyte. Cyclic Voltammetries where recorded with a potential step of 0.008 V and a scan rate of 0.1 V/s, Impedance Spectroscopy was recorded between 65000 Hz and 0.1 Hz with an amplitude of 0.01 V_{RMS}. Photoelectrochemistry was evaluated using a 500 W UV Lamp [HG 500] from Jelosil and LEDs (M395 L4, M455 L4, and the LEDD1B power supply) from Thorlabs.

Conflict of Interest

The authors declare no conflict of interest.

Data Availability Statement

The data that support the findings of this study are available from the corresponding author upon reasonable request.

[1] W. W. Zhao, J. J. Xu, H. Y. Chen, *Analyst* **2016**, *141*, 4262–4271.
[2] Q. Liu, H. Zhang, H. Jiang, P. Yang, L. Luo, Q. Niu, T. You, *Biosens. Bioelectron.* **2022**, *216*, 114634.
[3] L. Neven, H. Barich, N. Sleegers, R. Cánovas, G. Debruyne, K. De Wael, *Anal. Chim. Acta* **2022**, *1206*, 339732.
[4] M. Petruleviciene, J. Juodkazyte, I. Savickaja, R. Karpicz, I. Morkvenaite-Vilkonciene, A. Ramanavicius, *J. Electroanal. Chem.* **2022**, *918*, 116446.
[5] B. Bastug Azer, A. Gulsaran, J. R. Pennings, R. Saritas, S. Kocer, J. L. Bennett, Y. Devdas Abhang, M. A. Pope, E. Abdel-Rahman, M. Yavuz, *J. Electroanal. Chem.* **2022**, *918*, 116466.
[6] F. Bakhshandeh, S. Saha, S. Sakib, I. Zhitomirsky, L. Soleymani, *J. Electrochem. Soc.* **2022**, *169*, 057520.
[7] H. Geng, X. Chen, L. Sun, Y. Qiao, J. Song, S. Shi, Q. Cai, *Anal. Chim. Acta* **2021**, *1146*, 166–173.
[8] S. Sheng, Z. Zhang, M. Wang, X. He, C. Jiang, Y. Wang, *Electrochim. Acta* **2022**, *420*, 140441.
[9] Z. Yang, W. Xu, B. Yan, B. Wu, J. Ma, X. Wang, B. Qiao, J. Tu, H. Pei, D. Chen, Q. Wu, *ACS Omega* **2022**, *7*, 2474–2483.
[10] P. Gao, H. Ma, J. Yang, D. Wu, Y. Zhang, B. Du, D. Fan, Q. Wei, *New J. Chem.* **2015**, *39*, 1483–1487.
[11] J. Zhao, J. Cheng, Y. Sun, J. Liu, W. Chen, Y. Xu, J. Yang, Y. Li, *Microchimica Acta* **2021**, 188.
[12] L. Shi, Y. Yin, L. C. Zhang, S. Wang, M. Sillanpää, H. Sun, *Appl. Catal. B* **2019**, *248*, 405–422.
[13] H. Cheng, X. Wang, Z. Bai, C. Zhu, Z. Zhang, Q. Zhang, Q. Wang, H. Dong, B. Xu, *Nanotechnology* **2023**, *34*, 015703.
[14] M. Zanatta, L. Calvillo, J. Zheng, G. A. Rizzi, G. Durante, G. Giallongo, D. Chirkov, L. Colazzo, C. Marega, A. Gennaro, G. Granozzi, *Thin Solid Films* **2016**, *603*, 193–201.
[15] Y. He, Z. Ren, L. Yan, J. Liu, L. A. Belfiore, J. Tang, S. Mao, *Appl. Surf. Sci.* **2022**, *605*, 154768.
[16] M. V. Dozzi, A. Candeo, G. Marra, C. D'Andrea, G. Valentini, E. Selli, *J. Phys. Chem. C* **2018**, *122*, 14326–14335.
[17] Y. Jiang, Q. Li, J. Yao, X. Guo, Y. Ying, X. Liu, Y. Wen, H. Yang, Y. Wu, *Appl. Surf. Sci.* **2022**, *581*, 151903.
[18] S. Saha, J. Yang, S. S. M. Masouleh, G. A. Botton, L. Soleymani, *Electrochim. Acta* **2022**, *404*, 139746.
[19] A. B. Tesler, T. Sannomiya, S. Hejazi, R. Mohammadi, N. Vogel, M. Altomare, P. Schmuki, *Nano Energy* **2021**, *90*, 106609.
[20] M. Khairy, E. M. Kamar, M. A. Mousa, *Mater. Sci. Eng. B* **2022**, *286*, 116023.
[21] L. Cao, Z. Li, R. Jia, L. Chen, Y. Wu, J. Di, *Anal. Lett.* **2020**, *53*, 1472–1488.
[22] L. Xu, H. Li, P. Yan, J. Xia, J. Qiu, Q. Xu, S. Zhang, *J. Colloid Interface Sci.* **2016**, *483*, 241–248.
[23] P. Yan, L. Xu, D. Jiang, H. Li, J. Xia, Q. Zhang, M. Hua, *Electrochim. Acta* **2018**, *259*, 873–881.
[24] L. Xu, P. Yan, H. Li, S. Ling, J. Xia, J. Qiu, Q. Xu, H. Li, S. Yuan, *Mater. Lett.* **2017**, *196*, 225–229.
[25] P. Yan, J. Dong, Z. Mo, L. Xu, J. Qian, J. Xia, J. Zhang, H. Li, *Biosens. Bioelectron.* **2020**, *148*, 111802.
[26] A. A. R. Herizchi, E. Abbasi, M. Milani, *Artif. Cells, Nanomedicine, Biotechnol.* **2016**, *44*, 596–602.
[27] V. Pifferi, G. Soliveri, G. Panzarasa, S. Ardizzone, G. Cappelletti, D. Meroni, L. Falciola, *RSC Adv.* **2015**, *5*, 71210–71214.
[28] G. Soliveri, V. Pifferi, G. Panzarasa, S. Ardizzone, G. Cappelletti, D. Meroni, K. Sparnacci, L. Falciola, *Analyst* **2015**, *140*, 1486–1494.
[29] V. Pifferi, G. Soliveri, G. Panzarasa, G. Cappelletti, D. Meroni, L. Falciola, *Anal. Bioanal. Chem.* **2016**, *408*, 7339–7349.
[30] R. G. Compton, C. E. Banks, *Understanding Voltammetry*, **2018**.
[31] X. Hu, X. Hu, Q. Peng, L. Zhou, X. Tan, L. Jiang, C. Tang, H. Wang, S. Liu, Y. Wang, Z. Ning, *Chem. Eng. J.* **2020**, *380*, 122366.
[32] T. An, H. Yang, G. Li, W. Song, W. J. Cooper, X. Nie, *Appl. Catal. B* **2010**, *94*, 288–294.
[33] G. Maino, D. Meroni, V. Pifferi, L. Falciola, G. Soliveri, G. Cappelletti, S. Ardizzone, *J. Nanopart. Res.* **2013**, 15.
[34] G. Di Liberto, V. Pifferi, L. Lo Presti, M. Ceotto, L. Falciola, *J. Phys. Chem. Lett.* **2017**, *8*, 5372–5377.

RESEARCH ARTICLE
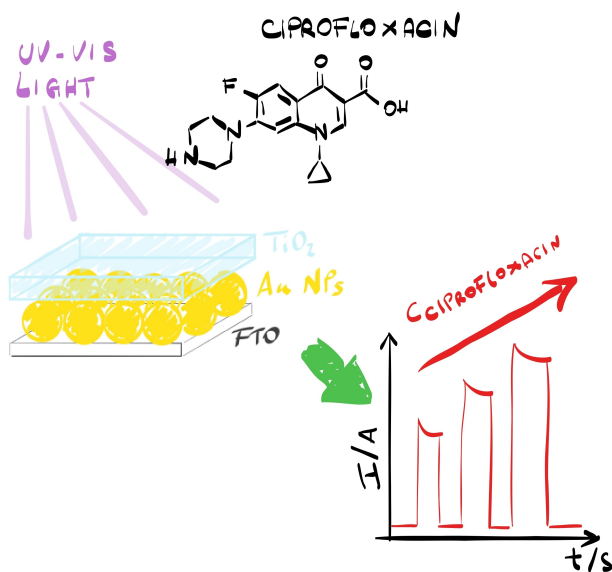
D. Fumagalli, S. Comis, Prof. V. Pifferi*, Prof. L. Falciola*

1 – 9

Gold Nanoparticles-Titania Heterojunction: Photoelectrochemical Detection of Ciprofloxacin

Photoelectrochemical detection of ciprofloxacin: A heterojunction formed by titanium dioxide and gold nanoparticles can determine ciprofloxacin by photoelectrochemical analysis. Thanks to the synergistic properties of the two materials, it is possible to use low-power and visible light sources and limit interferences.